Specific Tryptophan UV-Absorbance Changes Are Probes of the Transition of Rhodopsin to Its Active State†

Steven W. Lin and Thomas P. Sakmar*

Howard Hughes Medical Institute, Laboratory of Molecular Biology and Biochemistry, The Rockefeller University, 1230 York Avenue, New York, New York 10021

Received April 10, 1996; Revised Manuscript Received June 17, 1996⊗

ABSTRACT: The difference of rhodopsin and metarhodopsin II (MII) absorption spectra exhibits a characteristic pattern in the UV wavelength range, consisting of peaks at 278, 286, 294, and 302 nm. These difference bands are thought to result from the perturbation of the environments of tryptophan and/or tyrosine residues. We used site-directed mutagenesis to investigate the contribution of tryptophan absorption to these spectral features. Each of the five tryptophan residues in bovine rhodopsin was replaced by either a phenylalanine or a tyrosine. The mutant pigments (W35F, W126F, W161F, W175F, W265F/Y) were prepared and studied by UV−visible photobleaching difference spectroscopy. The difference spectra of the W35F and W175F mutants were identical to that of rhodopsin, whereas in the W161F mutant, the magnitudes of the 294- and 302-nm bands were slightly lowered. The differential absorbance at 294 nm was reduced by over 50% in the W126F and W265F/Y mutants. The difference peak at 302 nm was reduced in the W265F/Y mutants, but was almost completely absent in the W126F mutant. These data indicate that the difference bands at 294 and 302 nm originate from the perturbations of Trp^{126} and Trp^{265} environments resulting from a general conformational change concomitant with MII formation and receptor activation. Model studies on tryptophan absorption indicate that the difference peak at 294 nm is due to the differential shift of the L_b absorption of the indole side chain as a result of decreased hydrophobicity or polarizability of the Trp^{126} and Trp^{265} environments. The resolution of the 302-nm band, assigned to the differential shift of the indole L_a absorption, is consistent with hydrogen-bonding interactions of the indole N-H groups of Trp^{126} and Trp^{265} becoming weaker in MII. These results suggest that the photoactivation of rhodopsin involves a change in the relative disposition of transmembrane helices 3 and 6, which contain Trp^{126} and Trp^{265} respectively, within the α-helical bundle of the receptor.

Rhodopsin, the visual pigment of the rod cell, is a member of a superfamily of seven-transmembrane helix receptors (Khorana, 1992). Photoactivated rhodopsin catalyzes GDP/GTP exchange in the visual G protein, transducin. The 11-*cis*-retinal chromophore in bovine rhodopsin is covalently linked by a protonated Schiff base (PSB)[1] bond to Lys^{296} (Figure 1). Glu^{113} functions as the counterion and stabilizes the positive charge of the PSB group (Sakmar et al., 1989; Zhukovsky & Oprian, 1989; Nathans, 1990). The light-induced isomerization of the chromophore to the *all-trans* geometry initiates the conversion of the chromophore−opsin complex via several spectrally distinct intermediates to the active R* state. During the transition from metarhodopsin I (MI, λ_{max} = 480 nm) to metarhodopsin II (MII, λ_{max} = 380 nm), the chromophore deprotonates and the opsin adopts the active conformation. This R* state is defined by a change in the structures of the loop domains on the cytoplasmic surface to conformations that are capable of binding and activating transducin. Mutagenesis and peptide competition studies point to the interaction of cytoplasmic loops 2 (helix 3−4 loop) and 3 (helix 5−6 loop) with transducin (Franke et al., 1990, 1992; Ernst et al., 1995; Hamm et al., 1988; Resek et al., 1994).

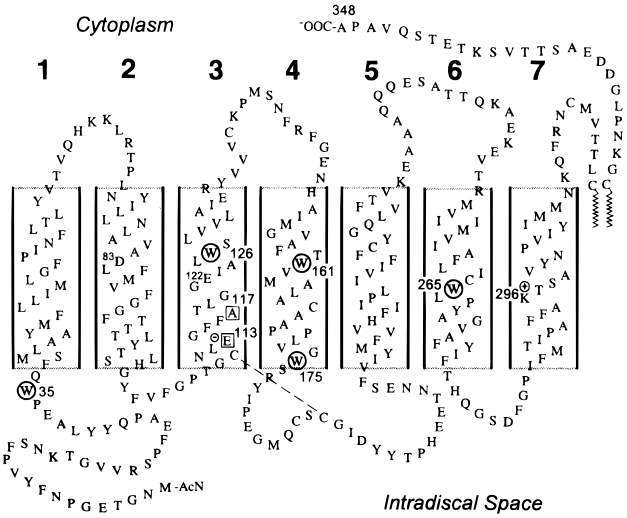

FIGURE 1: Secondary structural model of bovine rhodopsin. The five tryptophan residues in the primary structure are circled.

† S.W.L. is an Associate and T.P.S. is an Associate Investigator of the Howard Hughes Medical Institute.

* To whom correspondence may be addressed at: Box 284, Rockefeller University, 1230 York Ave., New York, NY 10021. Email: sakmar@rockvax.rockefeller.edu; Tel: 212-327-8288; Fax: 212-327-7904.

⊗ Abstract published in *Advance ACS Abstracts,* August 1, 1996.

[1] Abbreviations: bp, base pairs; DMSO, dimethyl sulfoxide; ϵ_{max}, molar extinction at the absorption maximum; $\Delta\epsilon$, change in molar extinction; EPR, electron paramagnetic resonance; FTIR, Fourier-transform infrared; λ_{max}, absorption maximum; MI, metarhodopsin I; MII, metarhodopsin II; NATA, *N*-acetyl-L-tryptophanamide; PSB, protonated Schiff base; R and R*, inactive and active receptor conformation, respectively; ROS, rod outer segment; UV, ultraviolet.

S0006-2960(96)00858-6 CCC: $12.00

The transduction of the signal (i.e., light absorption) from the interior of the receptor to the surface loops is presumably accomplished by a modification of its transmembrane structure. The FTIR spectra of the thermal intermediates in the bleaching of rhodopsin exhibit changes in the amide vibrations that are consistent with a conformational transition involving the alterations of helix backbone structures (Klinger & Braiman, 1992; Garcia-Quintana et al., 1995). Perturbations of the hydrogen-bonding interactions of Glu^{122}(Fahmy et al., 1993), Asp^{83} (Fahmy et al., 1993; Rath et al., 1993), and cysteine residue(s) (Rath et al., 1994) and the protonation of Glu^{113} (Jäger et al., 1994) have also been detected by FTIR spectroscopy. EPR spectroscopy on site-specific spin-labeled rhodopsin mutants suggests movement of residues on the cytoplasmic border of helix 3 during receptor activation (Farahbakhsh et al., 1995).

There is evidence that the local protein environments around tryptophan residues change during the thermal conversion of rhodopsin to MII. The difference spectrum obtained by subtracting the UV−visible absorption spectra of MII and rhodopsin shows distinct peaks at 278, 286, 294, and 302 nm. Since these wavelengths are close to the lowest $\pi-\pi^*$ optical transitions of a tryptophan, Rafferty and coworkers (1980) interpreted these UV-difference bands in terms of the environments of at most two tryptophan residues becoming more polar in MII. In addition, a linear dichroism study of these bands by Chabre and Breton (1979) indicated a reorientation of an indole side chain during the MI → MII conversion. There are a total of five tryptophan residues (positions 35, 126, 161, 175, and 265) in the primary structure of bovine rhodopsin, three of which (Trp^{126}, Trp^{161}, and Trp^{265}) reside in the putative membrane-embedded portion of the opsin (Figure 1). The tryptophan residues at positions 126, 161, and 175 are conserved in virtually all vertebrate rhodopsins and cone visual pigments (Yoshizawa, 1992). Trp^{265} is conserved in all pigments, except in the family of blue cone pigments in which the residue is a tyrosine. A tryptophan is also conserved at position 35 except in the blue cone pigments of some species (e.g., chicken, goldfish). The red and green cone pigments contain additional tryptophan residues, whose conservation is variable between species.

A tryptophan is often used as a noninvasive environment-sensitive probe of protein structure because of its unique absorption and fluorescence properties. Structural studies of bovine rhodopsin and its intermediates by fluorescence spectroscopy of tryptophan residues have been impractical because of the low fluorescence quantum yield (∼0.022) apparently due to quenching by the retinal chromophore via energy transfer (Ebrey, 1972). In one study, however, this property was exploited and served as a basis for monitoring MII decay by measuring the fluorescence increase due to the release of free retinal out of the opsin after Schiff base hydrolysis (Farrens & Khorana, 1995). In this paper, we report the preparation and the biophysical characterization of tryptophan mutants of bovine rhodopsin for the purpose of assigning the UV-difference absorption bands to specific tryptophan residues. These assignments, coupled with model studies on tryptophan absorption, are used to interpret the absorbance changes in terms of the perturbations of the local tryptophan environments and of the general opsin structure, which occur during the activation of the receptor.

MATERIALS AND METHODS

Reagents. Monoclonal antibody 1D4 was prepared by the National Cell Culture Center (Minneapolis, MN). The 11-*cis*-retinal was provided by the National Eye Institute through Dr. Rosalie Crouch. NATA was purchased from Sigma (St. Louis, MO). Sources of other reagents were previously reported (Min et al., 1993; Zvyaga et al., 1993; Chan et al., 1992)

Construction and Expression of Rhodopsin Mutants. Site-directed mutagenesis was performed using restriction fragment replacement "cassette mutagenesis" in a synthetic gene for rhodopsin that had been cloned into the expression vector as previously described (Min et al., 1993; Franke et al., 1988). DNA oligonucleotides containing the desired codon alterations were synthesized on an Applied Biosystems Model 392 DNA synthesizer, and then purified and annealed. The mutagenic duplexes for the mutants were as follows: W35F, 129-bp *Kpn*I−*Bcl*I duplex; W126F, 62-bp *Rsr*II−*Spe*I duplex; W161F, 114-bp *Spe*I−*Sfi*I duplex; W175F, 24-bp *Sfi*I−*Xba*I duplex; W265F/Y, 95-bp *Mlu*I−*Apa*I duplex. The duplex for E113A/A117E was prepared as previously reported (Zvyaga et al., 1994). The nucleotide sequences of all cloned synthetic duplexes were confirmed by the chain terminator method for DNA sequencing on purified plasmid DNA using Sequenase Ver 2.0 (United States Biochemical). The altered genes were expressed in COS-1 cells following transient transfection by a lipofectamine procedure (GIBCO BRL, Life Technologies).

Reconstitution and Purification of Mutant Pigments. COS cells expressing mutant apoprotein were harvested ∼40 h after transfection and incubated in the presence of 11-*cis*-retinal (∼80 μM) at 4 °C under dim-red light to reconstitute a pigment. The pigment was solubilized in the dodecyl maltoside detergent (w/v 1%, 50 mM Tris-HCl, pH 7, 100 mM NaCl, 1 mM $CaCl_2$, 0.1 mM phenylmethanesulfonyl fluoride) and bound to the 1D4-immunoaffinity resin(Sakmar et al., 1989). The resin was washed four times with 10× bed volume of low-salt, low-pH wash buffer (2 mM phosphate buffer, pH 6, 0.1% (w/v) dodecyl maltoside or digitonin). The pigment was eluted by supplementing the wash buffer with the antigenic carboxyl-terminal peptide to the 1D4 antibody. The low salt and low pH of the buffer result in a preferential elution of the correctly folded pigment which had regenerated with 11-*cis*-retinal (Ridge et al., 1995). Aliquots of concentrated Tris-HCl and NaCl solutions were added to the eluted pigment to bring their final concentrations to 50 mM (pH 7) and 100 mM, respectively.

Absorption Spectroscopy. Spectroscopy was performed on a λ-19 Perkin-Elmer spectrophotometer. The sample (100 μL) was placed in a quartz cuvette (1-cm path length) which was kept at 3 °C. The sample chamber was purged with N_2(g) to prevent condensation. Absorption scans (∼50 scans) of the unphotolyzed pigment were collected first. To bleach the pigment, the sample was illuminated in the cuvette for 15 s, or longer if needed, with a 150-W halogen light source filtered through a 495-nm long-pass filter. Immediately afterward, 20−50 scans of the photolyzed pigment were recorded. The step size was 1 nm, and the spectral resolution was 2 nm.

The normalized difference spectrum for each pigment was calculated using the expression,

Table 1: Spectral Properties and Relative Transducin Activation Rates of Rhodopsin Mutants

pigment	λ_{max} (nm)	relative ϵ_{max} (±10%)[a]	relative transducin activation (±10%)[b]
rhodopsin	500	1.0	1.0
W35F	500	1.0	1.0
W126F	500	0.90	0.50
W161F	500	0.90	0.90
W175F	500	1.0	1.0
W265Y(F)	485 (481)	1.0	0.80
E113A/A117E @ pH 6	493	0.90	~0.53[c]

[a] The extinction coefficient of each pigment was determined by acid denaturation as described in Materials and Methods. [b] Initial rate of light-dependent activation of transducin by each pigment at pH 7.2 (5 °C) normalized by the rate of rhodopsin. [c] Calculated from data in Zvyaga et al. (1994). The relative transducin activation rates by rhodopsin and the E113A/A117E mutant are ~0.65 and 0.35, respectively, at pH 6.

$$\Delta(\text{absorbance}) = \frac{(L - D)}{(\text{absorbance @ } \lambda_{max})} \times \frac{1}{(\text{photoproduct yield})} \times \frac{(\epsilon_{max} \text{ of mutant})}{(\epsilon_{max} \text{ of rhodopsin})}$$

where L and D refer to the absorption spectrum of the pigment recorded after and before illumination, respectively. The first term expresses the difference as a fractional change relative to the initial pigment absorbance in the dark. It is normalized by the approximate fraction of the photoproduct in the photolyzed sample in order to scale its magnitude to the case of ~100% photoproduct formation. The photoproduct yield was estimated from its absorbance at λ_{max}. In the case of rhodopsin and tryptophan mutants, the photoproduct displayed a λ_{max} value of 380 nm. For rhodopsin in digitonin and the E113A/A117E mutant, the photoproduct was a species with λ_{max} value at ~475 nm. Multiplication by the ratio of the ϵ_{max} values corrects for the difference in pigment concentration between the mutant and rhodopsin samples. Δ(Absorbance) of 1.0 corresponds to a change in molar extinction of ~40 600 M^{-1} cm^{-1}.

Estimate of the Extinction Coefficient at λ_{max}. The ϵ_{max} of each pigment was determined from the ratio of its absorbance at λ_{max} in the dark and the absorbance at 440 nm of retinal PSB, which is produced when the pigment is acid denatured by the addition of HCl. The ϵ_{max} values of the mutant pigments relative to the value of rhodopsin are listed in Table 1. The ϵ_{max} of rhodopsin is ~40 600 M^{-1} cm^{-1} (Wald & Brown, 1953).

Assay of Light-Dependent Transducin Activation Rates. The radionucleotide filter-binding assay of light-dependent transducin activation by a pigment was carried out as described (Min et al., 1993; Zvyaga et al., 1994). Briefly, aliquots of the reaction mixture (4 nM pigment, 700 nM purified bovine transducin, 50 mM Tris-HCl, pH 7.3, 100 mM NaCl, 2 mM $MgCl_2$, 1 mM dithiothreitol, 0.01% dodecyl maltoside, 20 μM [^{35}S]GTPγS, 5 °C) were removed at constant time intervals during the assay and applied to nitrocellulose filters (Schleicher & Schuell, BA85). The relative amount of [^{35}S]GTPγS that bound irreversibly to transducin was quantitated by measuring the radioactivity of the filters in a scintillation counter. Background radioactivity was determined from aliquots removed from the reaction mixture in the dark. Light-dependent uptake of GTPγS by transducin was assayed under constant background illumination with light filtered through a 495-nm long-pass filter. The initial rate of transducin activation was estimated from a linear-regression fit to the data points obtained during the first minute of the illumination.

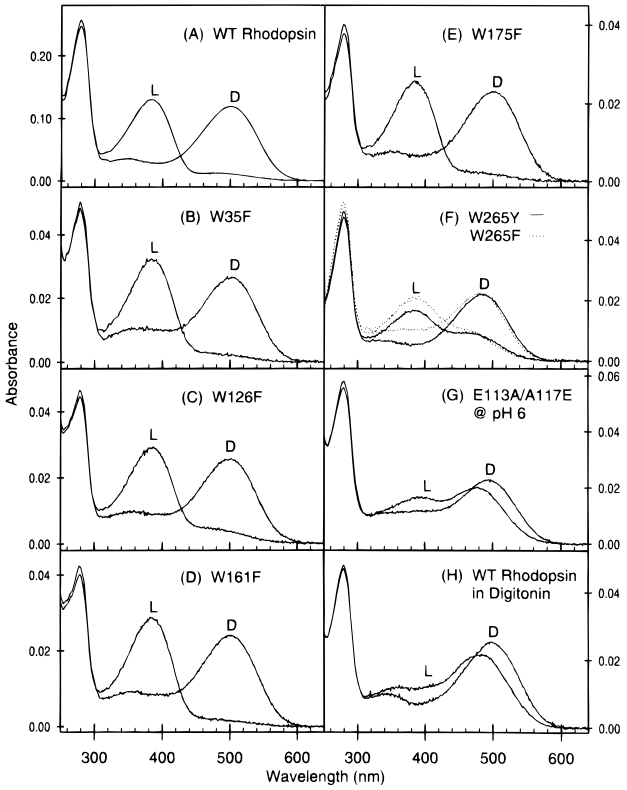

FIGURE 2: UV−visible absorption spectra of recombinant rhodopsin and mutant rhodopsins. (A) Rhodopsin, (B) W35F, (C) W126F, (D) W161F, (E) W175F, (F) W265Y and W265F, and (G) E113A/A117E pigments solubilized in dodecyl maltoside. (H) Rhodopsin solubilized in digitonin. For each pigment, the spectrum recorded before and after illumination by >495-nm light are labeled "D" and "L", respectively. All of the pigments were reconstituted in 0.1% dodecyl maltoside (A−G) except for one rhodopsin sample, which was reconstituted in 0.1% digitonin (H). Note that the spectra of both W265F and W265Y pigments are presented in a single panel (F). Spectra were taken through 1-cm path length at 3 °C.

RESULTS

UV−Visible Absorption of Rhodopsin. The absorption spectrum of rhodopsin consists of a broad band with a maximum at 500 nm and a narrower band with a maximum at ~280 nm (Figure 2A). The 500-nm band corresponds to the lowest energy electronic excitation of the 11-*cis*-retinal PSB chromophore in the pigment. The 280-nm line is a composite of the overlapping absorption bands of aromatic residues in the protein. There are 31 phenylalanine, 18 tyrosine, and 5 tryptophan residues in the rhodopsin primary structure. The ratio of the protein and chromophore absorptions (i.e., A_{280}/A_{500}) gives a relative measure of the extent of reconstitution of the opsin with 11-*cis*-retinal. Rhodopsin purified from bovine retina or from COS-1 cells typically has a ratio of 1.6−1.7. A ratio of 1.8 or greater is indicative of the presence of contaminating protein(s) or non-reconstituted opsin. Since the immunoaffinity purification procedure is selective for the visual opsin, the contaminating species in most cases is excess unreconstituted misfolded

opsin. However, the low-salt, low-pH elution condition employed in the purification minimizes the amount of unreconstituted opsin that coelutes with the pigment (Ridge et al., 1995).

The illumination of the rhodopsin solubilized in dodecyl maltoside converts nearly 100% of the ground-state pigment to MII. This reaction is characterized by the shift of the visible absorption band to 380 nm, which is caused by the deprotonation of the chromophore Schiff base. This shift is also accompanied by ~5% decrease of the absorbance at 280 nm. Over time, MII thermally decays to MIII (λ_{max} ~460 nm) and the Schiff base linkage between the retinal and Lys[296] is hydrolyzed to yield free *all-trans*-retinal (λ_{max} ~380 nm) and opsin (Hofmann, 1986). However, under the conditions employed in this study (3 °C, pH 7.0), MII is kinetically stable during the collection of the absorbance scans. We estimate that ~5% of MII converted to MIII based on the very small decrease of the absorbance at 380 nm and a corresponding increase at ~460 nm. To estimate the extent of Schiff base hydrolysis, the fraction of intact Schiff base linkage was assayed by denaturing the sample by the addition of HCl. The 440-nm absorbance of the retinal PSB generated by the denaturation of the photolyzed pigment at the end of the experiment was similar in magnitude to that obtained when unphotolyzed rhodopsin was acid denatured (data not shown). This indicates that most of the 380-nm absorbance was due to the absorption by the chromophore of MII and not due to free retinal. We estimate that the MII population decreased by ≤10% via the two pathways by the end of a typical experiment.

The "dark" spectrum was subtracted from the "light" spectrum to reveal spectral features that change between rhodopsin and MII. The visible region of the difference spectrum contains a positive band at 380 nm and a negative band at 500 which correspond to the absorption bands of the unprotonated and the protonated Schiff base chromophore in MII and rhodopsin, respectively (data not shown). In the UV wavelengths, the subtraction yields smaller, but reproducible differential absorbance peaks. The expanded view of the MII/Rho difference between 250 and 320 nm is shown in Figure 3A. The base line is approximated by extrapolating a Gaussian fit of the blue side of the 380-nm envelope to the region below 320 nm. The negative differential absorbance pattern between 270 and 320 nm is composed of at least four separate bands. There is a broad peak centered at 278 nm that overlaps with a narrower line at 286 nm. The differential absorbance at 278 nm corresponds to a change in molar extinction ($\Delta\epsilon$) of ~3000 M^{-1} cm^{-1}, and the $\Delta\epsilon$ at 286 nm is ~3500 M^{-1} cm^{-1}. Between 290 and 310 nm, there are two overlapping bands centered at 294 and 302 nm, each with $\Delta\epsilon$ of ~3500 M^{-1} cm^{-1}. Similar UV-difference features were observed in the MII/Rho spectrum of rhodopsin in native ROS membranes (Rafferty, 1979). The wavelengths of the difference peaks also generally agree with those in the light/dark difference spectrum of Emulphogene-solubilized rhodopsin (Rafferty et al., 1980), but the relative heights of the bands differ slightly.[2]

Solubilization of Rhodopsin in Digitonin. Rhodopsin reconstituted in digitonin displayed the same λ_{max} value as that of the pigment in dodecyl maltoside, but showed an altered bleaching process (Figure 2H). After illumination, the absorption peak shifted to ~480 nm and decreased in height, while the absorbance at ~380 nm increased slightly. The λ_{max} of 480 nm is characteristic of the MI species (Franke et al., 1992; Resek et al., 1994). The absorption spectrum shows that the thermal transition of MI to MII is inhibited in digitonin and that most of the pigment at 3 °C is trapped in the MI state.

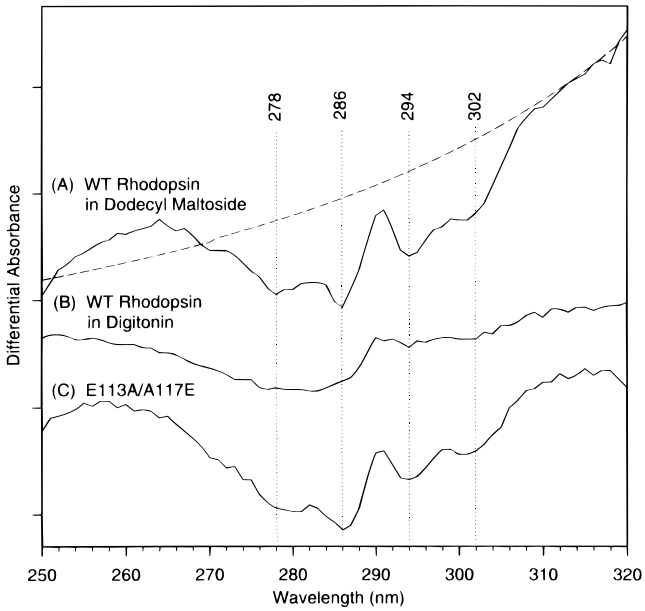

FIGURE 3: Normalized photobleaching-difference spectra (250−320 nm) of rhodopsin reconstituted in (A) 0.1% dododecyl maltoside and (B) 0.1% digitonin. (C) Normalized photobleaching-difference spectrum of the E113A/A117E mutant in dodecyl maltoside. The difference spectra are computed from the "D" and "L" spectra shown in Figure 2 (see Materials and Methods). The dashed line in (A) is the base line estimated by extrapolating the short-wavelength tail of the 380-nm peak to wavelengths below 320 nm. One interval on the ordinate is equivalent to a $\Delta\epsilon$ of ~4060 M^{-1} cm^{-1}.

Since the MI species is more abundant in the photolyzed pigment solubilized in digitonin, the subtraction of the "dark" spectrum from the "light" spectrum essentially yields a pure difference between MI and rhodopsin (Figure 3B). The sharp difference bands, which were observed in the MII/Rho spectrum, are absent in the MI/Rho spectrum. Instead, there is only a single broad featureless band at ~281 nm. The differential absorbance at 281 nm corresponds to $\Delta\epsilon$ of ≤2000 M^{-1} cm^{-1}, about a factor of 1.5 less than the $\Delta\epsilon$ values found in the MII/Rho spectrum. The comparison of the two difference spectra shows that difference bands at

[2] Specifically, the $\Delta\epsilon$ at 286 nm is ~2 times larger and the 294-nm band appears as an unresolved shoulder on a larger band at 300 nm in the light/dark difference spectrum of Rafferty et al. (1980). We ascribe these differences to the fact that the spectrum of illuminated rhodopsin obtained by Rafferty et al. is actually a spectrum of the denatured pigment. Their "light" spectrum was recorded ~1 h (@ 25 °C) after the rhodopsin had been photolyzed. Under this condition, no MII would likely be present. We observed similar spectral features in our samples that had been acid denatured, or that were photolyzed in the presence of hydroxylamine. In order to confirm that the differences were not due to effects associated with the specific interaction of the protein with the detergent, we also repeated the absorbance measurements on rhodopsin solubilized in the detergent Lubrol PX which has a hydrophobic tail that is chemically equivalent to Emulphogene BC720. The UV-difference features in the light/dark spectrum of Lubrol-solubilized rhodopsin recorded at 3 °C (data not shown) were identical to those of the MII/Rho spectrum reported in this study, except that the sizes of the bands were slightly smaller because the MI → MII conversion in Lubrol was not 100% complete.

278, 286, 294, and 302 nm with $\Delta\epsilon$ values of $\geq$3000 M^{-1} cm^{-1} are characteristic of the MII/Rho spectrum.

Mutant Pigment E113A/A117E. The E113A/A117E pigment in dodecyl maltoside absorbs maximally at 493 nm (Figure 2G and Table 1). The photolysis of the ground-state pigment produces a pH-dependent mixture of 474- and and 380-nm photoproducts, which contain protonated and unprotonated Schiff base chromophores, respectively. Earlier studies have shown that the 474-nm pigment, which predominates at acidic pH, is the active R* species that is capable of activating transducin (Zvyaga et al., 1994; Fahmy et al., 1994). The difference between the absorption spectrum of the ground-state and photolyzed pigment yields UV-spectral features that closely resemble those of the MII/Rho difference (Figure 3C). Specifically, the four difference bands are detected at 278, 286, 294, and 302 nm. These UV-difference bands are associated with the active 474-nm species because it is the main photoproduct when the buffer pH is 6.

Tryptophan Replacement Mutants. To determine if the UV-difference features of the MII/Rho spectrum were caused by perturbation(s) of tryptophan absorption, we repeated the absorption measurements on site-directed mutants of rhodopsin in which each of the five tryptophans in the sequence had been replaced by phenylalanine or tyrosine. The absorption spectra of the tryptophan mutants are presented in Figure 2B−F, and their biochemical properties are listed in Table 1. The λ_{max} values of the ground-state pigments in all of the mutants, except for W265F and W265Y, are unchanged from the λ_{max} of rhodopsin. The absorption bands of the W265 mutants are blue-shifted by ~20 nm. The λ_{max} values of W126F, W265F, and W265Y pigments are identical to those previously reported by Khorana and coworkers (Ridge et al., 1992; Nakayama & Khorana, 1991). The $A_{280}/A_{\lambda_{max}}$ ratio of the mutant preparations varied between ~1.7 and ~2.0, indicating that their purities were comparable to that of a typical rhodopsin preparation. However, compared to rhodopsin purified from COS cells transfected in parallel, the absolute amount of some of the tryptophan mutant pigments recovered using low-pH, low-salt elution buffer was consistently lower, indicating that these mutant opsins did not regenerate with 11-*cis*-retinal as well as the native opsin. The reconstitution yield was ~80% for the W161F and W265F/Y opsins and ~60% for the W126F opsin.

The W35F, W161F, and W175F mutants showed the same response to illumination as rhodopsin. There was a nearly complete shift of the 500-nm band to 380 nm, presumably due to the formation of MII-like species (Figure 2B,D,E). Consistent with this, these three pigments showed normal transducin activation rates (Table 1). In the W126F mutant, most of the ground-state species converted to the 380-nm species, but there appeared to be a small amount (<10%) of MI in equilibrium, as judged by some residual absorbance at ~480 nm (Figure 2C). The transducin activation rate by the photolyzed W126F pigment was ~50% of the rhodopsin rate. The production of MII-like species was further perturbed in the W265F and W265Y mutants. The illumination time that was required to completely bleach the other pigments only resulted in the formation of about half as much MII-like pigment for the W265F/Y mutants. About 60 s of illumination was required to convert the majority of the ground-state population in these two mutants to the 380-nm species (Figure 2F). The relative transducin activation rates of the photolyzed W265F/Y mutants were ~80% of the normal value. This number is close to the approximate fraction of the MII-like species present in the photolyzed samples as judged by their absorption spectra. We conclude that the MII-like spectral forms of the W265F/Y mutants are able to activate transducin at the same rate as MII of rhodopsin. Moreover, the acid denaturation of the photolyzed mutant pigments at the end of the scans yielded absorption bands characteristic of retinal PSB, which were similar to that obtained with the denaturation of rhodopsin (data not shown). This assay indicates that the relative amount of free retinal and/or MIII-like species in the photolyzed mixture of all tryptophan mutants was also ≤10%.

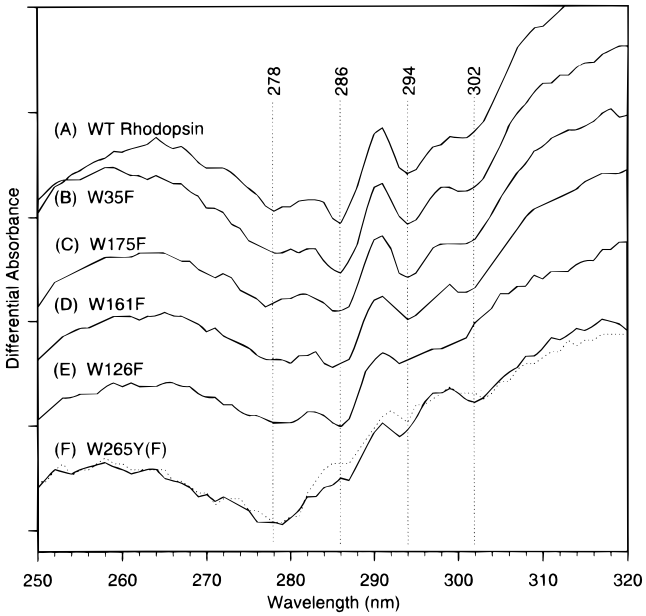

FIGURE 4: Normalized photobleaching-difference spectra of tryptophan mutants in 0.1% dodecyl maltoside. (A) Rhodopsin, (B) W35F, (C) W175F, (D) W161F, (E) W126F, and (F) W265Y (—) and W265F (···) pigments. The difference spectra are computed from the "D" and "L" spectra shown in Figure 2 (see Materials and Methods). One interval on the ordinate is equivalent to a $\Delta\epsilon$ of ~4060 M^{-1} cm^{-1}.

The light/dark difference spectra of the tryptophan mutants are presented in Figure 4. The spectra of the W35F and W175F mutants appear identical to the MII/Rho spectrum within the resolution and the signal-to-noise of the data. This is also clearly demonstrated in Figure 5, which displays the difference between the light/dark difference spectra of the mutant pigment and rhodopsin. This double-difference spectrum shows the loss of the UV-differential absorbance signal resulting from the tryptophan replacement and corresponds to the difference of the individual tryptophan absorbance between MII and the ground state, assuming that each mutation does not influence the remaining tryptophan absorptions. It is readily apparent that there is no differential absorbance due to either Trp^{35} or Trp^{175} between 270 and 320 nm. The replacement of Trp^{161} does not affect the overall shape of the difference features, but reduces the magnitudes of the 294- and 302-nm peaks by ~25%. By contrast, the substitutions of tryptophan at positions 126 and 265 elicit distinct changes to the shape and the size of the difference features (Figure 4E,F). For the W126F mutant, the magnitude of the peaks at 294 and 302 nm are ~50%

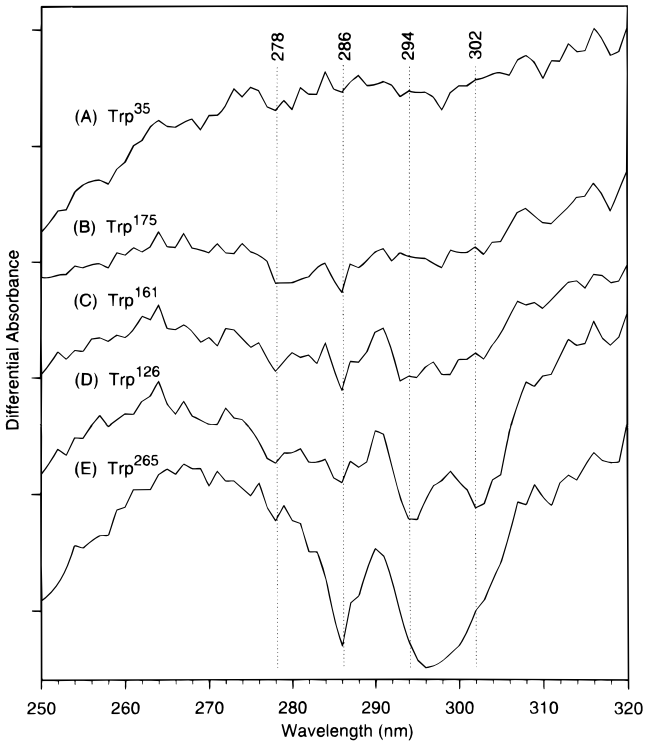

FIGURE 5: The difference spectrum of each individual tryptophan residue obtained by subtracting the photobleaching-difference spectrum of each tryptophan mutant pigment from the rhodopsin difference spectrum. Difference absorption spectrum of (A) Trp^{35}, (B) Trp^{175}, (C) Trp^{161}, (D) Trp^{126}, and (E) Trp^{265} between rhodopsin and MII. One interval on the ordinate is equivalent to $\Delta\epsilon$ of ~2030 M^{-1} cm^{-1}.

lower, but the features at 278 and 286 nm appear unchanged. The replacement of Trp^{265} causes a more general perturbation. It decreases the differential absorbance at 286 nm and the differential absorbance between 290 and 320 nm. However, clearly discernible peaks remain at ~293 and 302 nm. The difference spectra of Trp^{126} and Trp^{265} correspondingly show distinctive patterns (Figure 5D,E). The Trp^{126} difference spectrum consists of two overlapping bands at 294 and 302 nm, each with $\Delta\epsilon$ of ~2000 M^{-1} cm^{-1}. The difference spectrum of Trp^{265} has a sharp line at 286 nm and a broad asymmetric band with an $\Delta\epsilon$ of ~3000 M^{-1} cm^{-1} at ~296 nm.

DISCUSSION

In rhodopsin, the conversion of the pigment to MII results in ~5% decrease of the protein absorbance at 280 nm. The difference spectrum calculated by subtracting the absorption spectra of MII and rhodopsin displays a characteristic UV-spectral pattern, which consists of four overlapping downward-pointing bands with their peaks at 278, 286, 294, and 302 nm (Figure 3). These features are not observed in the MI/Rho spectrum. The shapes and the relative sizes of the difference bands in the MII/Rho and MI/Rho spectra of rhodopsin solubilized in detergent are similar to those seen in the difference spectra of rhodopsin in ROS membranes obtained under conditions that stabilized MII and MI, respectively (Rafferty, 1979).

A nonzero differential absorbance reflects the fact that the absorption spectrum of a residue has changed during the transition of rhodopsin to MII because of perturbation to its structure and/or environment. Therefore, the absence of any large difference features in the MI/Rho spectrum indicates that the opsin structures of rhodopsin and MI are not very different. To be precise, the thermal relaxation of the opsin structure following the *cis*−*trans* isomerization of the retinal chromophore does not involve significant reorganization (i.e., to a degree that influences the side-chain absorption spectrum) of the environments around the side chains responsible for the UV-difference bands. This result, combined with the fact that difference features are present in the MII/Rho spectrum, shows that the perturbations of the side-chain environments occur specifically during the MI → MII transition. The conversion of MI to MII consists of two sequential chemical events: (1) the deprotonation of the PSB group, and (2) the change of the protein conformation from its inactive form to the active R* state, which is able to bind transducin and to catalyze its GDP/GTP exchange (Arnis & Hofmann, 1993). *A priori*, the UV-difference bands may be reporting on environmental perturbation associated with either one of the processes.

In order to determine whether the UV-spectral changes can be ascribed to a specific event, the difference spectrum of the E113A/A117E mutant was examined. In this mutant, the counterion position on helix 3 has been moved up by 1 turn toward the cytoplasmic surface (Zvyaga et al., 1993). This mutation confers catalytic activity to the 474-nm photoproduct, which contains an *all-trans* chromophore with a *protonated* Schiff base. The visible absorption of this "active" photoproduct is similar to that of native MI, but the protein has adopted the R* conformation normally associated with active MII as assayed by its ability to activate transducin (Zvyaga et al., 1994) and by its FTIR spectrum (Fahmy et al., 1994). The net effect of this mutation is to decouple the Schiff base deprotonation from the conformational change required for receptor activation. We find that the difference between the 474-nm photoproduct and ground-state spectra of the E113A/A117E pigment displays the same UV-spectral features seen in the MII/Rho difference spectrum (Figure 3C). Since the Schiff base is still protonated, we conclude these UV-absorbance changes must originate from residues whose environments are altered specifically during the R → R* conformational transition. The UV-difference data of MII, MI, and the E113A/A117E pigment, taken together, also argue against the potential contribution from the UV absorption of the retinal chromophore to the observed difference features because neither the isomerization nor the deprotonation event which may be expected to change the absorption spectra of the 11-*cis* and *all-trans* chromophores is correlated with the appearance of the UV-difference bands.

Tryptophan Contribution to the UV Absorption. Only aromatic amino acids have side chains with significant molar extinction between 270 and 300 nm. Results from two earlier studies of native rhodopsin suggested that the UV-difference feature, specifically the bands at 294 and 302 nm, were due to the absorption by one or two tryptophans. Rafferty et al. (1980) were able to mimic the general bandshape and size of the difference peaks in their light/dark spectrum of solubilized rhodopsin by taking a difference between an absorption spectrum of tryptophan dissolved in water and one that had been artificially red-shifted in wavelength by 10 nm. The latter red-shifted spectrum was meant to mimic a spectrum of a tryptophan in a nonpolar solvent. A similar fitting analysis of the 286-nm band suggested that it could arise from the differential absorbance

of approximately 4 tyrosine residues. In a linear dichroism study of the bovine and frog MII/Rho spectra, Chabre and Breton (1979) showed that the dichroism of the UV-difference feature between 285 and ~300 nm resembled the dichroism of the tryptophan $\pi-\pi^*$ transitions inferred from its fluorescence polarization excitation spectrum. The assignment of the 294-nm difference band to a tryptophan absorbance in the two studies suggested that the environment of one or two tryptophans, which was initially apolar in rhodopsin, became polar or less apolar in MII.

In the present study, we employed site-specific mutagenesis to examine the contribution of tryptophan absorbance to the UV-difference bands in the MII/Rho difference spectrum. The replacement of Trp^{35} or Trp^{175} with phenylalanine had no effect on the spectroscopic and transducin-activation properties of the mutant pigments W35F and W175F. The UV-difference bands of these mutants were also identical to those of rhodopsin. Therefore, neither residue is responsible for absorbance changes between 280 and 300 nm, and the local environments of Trp^{35} and Trp^{175} are not altered during tertiary changes associated with the R → R* conversion. These results are not surprising given that transducin binds to the cytoplasmic surface of rhodopsin. Trp^{35} and Trp^{175} are located at the intradiscal ends of helices 1 and 4, respectively, and are possibly exposed to the solvent.

The three remaining tryptophan residues at positions 126, 161, and 265 are located in the transmembrane regions of helices 3, 4, and 6, respectively. The replacement of Trp^{161} results in a small decrease in the magnitude of the 294- and 302-nm difference bands, but the general spectral pattern is similar to that seen in rhodopsin. In contrast, the replacement at the 126 or 265 position causes significant perturbation of the UV-difference signal. In the W126F mutant, the difference lines at 294 and 302 nm are replaced by a broad unresolved feature with $\Delta\epsilon$ of ~1500 M^{-1} cm^{-1}. The substitution by phenylalanine or tyrosine at the 265 positions results in the decrease of the differential absorbance at 286 and 294 nm,[3] but does not seem to affect the signal at 302 nm. These data indicate that the difference features in the MII/Rho spectrum between 290 and 320 nm are caused by the differential absorbances of Trp^{126} and Trp^{265}. Trp^{265} makes the dominant contribution to the absorbance at 294 nm, but the 302-nm peak seems to be solely due to Trp^{126}. The difference band at 286 nm also disappears in the W265F/Y mutants, suggesting that it may also be due to Trp^{265} absorption. However, differential absorbances by several tyrosine residues most likely account for the majority of this signal because the size of this peak is not consistent with the molar extinction change of a single tryptophan (see below).

Given the evidence that the UV-difference features are specific to the R → R* process of the MI → MII transition, the results from the tryptophan mutant experiments show that the receptor activation alters the environments of Trp^{126} and Trp^{265}. The downward deflection of the 294- and 302-nm bands indicates that the absorption spectra of these tryptophans are red-shifted in rhodopsin compared to those in MII (Figure 5D, E). Since the red shift of a tryptophan absorption is correlated with its surroundings becoming more nonpolar and polarizable, the band assignments imply that Trp^{126} and Trp^{265} are initially in an environment that is solvent inaccessible, consistent with their putative locations in the membrane-spanning domain of the opsin (Figure 1). In MII, or more specifically the R* conformation, the environments of Trp^{126} and Trp^{265} become less nonpolar. Trp^{161}, which is also located in the low dielectric transmembrane domain, is expected to display a red-shifted absorption similar to that of Trp^{126} or Trp^{265}. However, the dielectric character and the polarizability of its environment apparently do not change significantly between R and R* conformations because the $\Delta\epsilon$ of the Trp^{161} difference is comparatively smaller (Figure 5C).

A similar perturbation of tryptophan environment has been inferred from transient UV absorbance at 296 nm in bacteriorhodopsin, a bacterial seven-transmembrane helix protein that contains a lysine-bound retinal prosthetic group. Absorption of light triggers a cyclic reaction consisting of several thermal intermediates, which are distinguished by different retinal configurations and/or protein conformational states (for review, see Mathies et al., 1991). In bacteriorhodopsin, the absorbance increase at 296 nm associated with the transition of the protein from the ground state to the conformationally-altered "M" intermediate (Hess & Kuschmitz, 1979; Sabés et al., 1984) has been assigned to the absorption of Trp^{182} (Wu et al., 1991). This residue resides near the chromophore on helix 6 of bacteriorhodopsin (Henderson et al., 1990), at a position analogous to Trp^{265} in rhodopsin.

Electronic Origin and Interpretation of the UV-Difference Bands. The lowest UV-absorption spectrum of the indole chromophore of tryptophan and the model compound NATA (Figure 6) is a superposition of two overlapping $\pi-\pi^*$ transitions designated L_a and L_b (Valeur & Weber, 1977; Albinsson et al., 1989). The overall width of the absorption envelope is primarily due to the broad, featureless L_a band. The L_b band is slightly narrower and is characterized by the presence of structured vibronic features. In water, the peaks of L_b vibronic bands are visible at 280 and 288 nm. The latter peak corresponds to the 0−0 band. In an increasingly nonpolar or polarizable environment, there is a progressive decrease of both L_a and L_b transitions to lower energies. The lowering of the L_b energy is evident from the red shift of the vibronic peaks, and the decrease of the L_a energy is inferred from the shift of the blue edge of the absorption envelope. The 0−0 L_b band of NATA shifts from 288 nm in water to ~291 nm in a less polar solvent like ethanol or a nonpolar solvent such as dioxane (Figure 6A). The corresponding difference spectra of NATA in water and in these solvents show a negative peak at ~292 nm, due to the shifted difference of the 0−0 L_b band, with $\Delta\epsilon$ of at most 1000 M^{-1} cm^{-1}, which returns to base line above 295 nm (Figure 6B). These NATA difference spectra can model the 294-nm difference peak in the MII/Rho spectrum, but do not satisfactorily reproduce the differential absorbance observed at ~300 nm.

[3] Given the assignment of the 294-nm difference band to Trp^{265}, a substitution of a tyrosine at this location should result in the appearance of a downward-pointing difference band between 285 and 290 nm. The $\Delta\epsilon$ of a difference band due to one tyrosine changing from a relatively nonpolar to polar environment (e.g., DMSO to water) is estimated to be ~700 M^{-1} cm^{-1}. There is no readily discernible peak in the W265Y spectrum that is assignable to a shifted tyrosine band, apparently due to its anticipated small size. However, the comparison of the W265Y and W265F spectra indicates a slightly larger differential signal at ~285 nm in the W265Y spectrum with the expected magnitude. We ascribe this shoulder to the shifted tyrosine difference band.

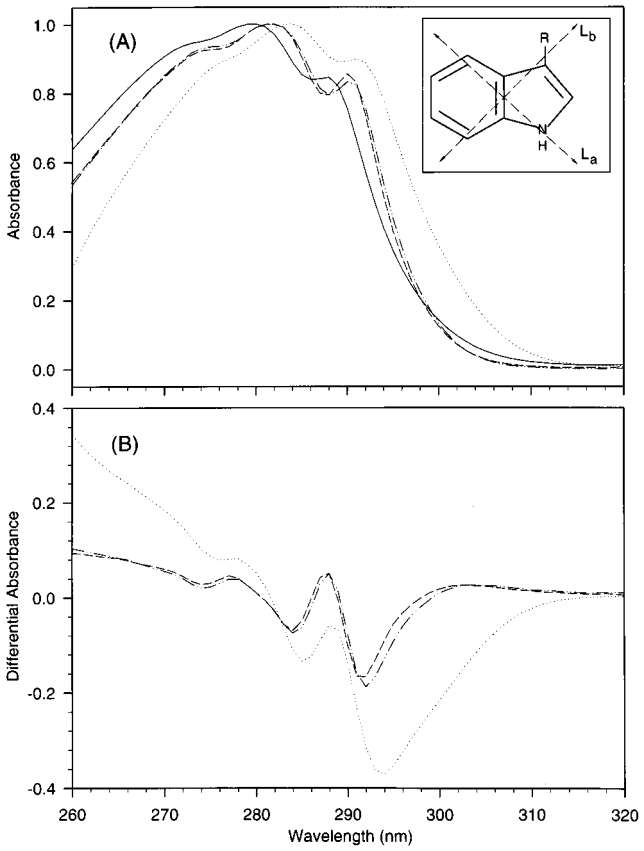

FIGURE 6: (A) Normalized absorption spectra of *N*-acetyl-L-tryptophanamide (NATA) dissolved in water (—), ethanol (---), DMSO (···), and dioxane (—··—). The ϵ_{max} at ~280 nm is ~5000 M^{-1} cm^{-1}. *Inset*: The indole chromophore of NATA. The angle between the L_a and L_b transition moments is ~90° (Albinsson et al., 1989). (B) Difference between NATA absorption in water and its absorption in ethanol (---), DMSO (···), and dioxane (—··—).

A model difference spectrum that more closely resembles the experimental curves is obtained when one subtracts the NATA spectrum in DMSO from that in water or ethanol (Figure 6B). The larger differential absorbance around 300 nm is a result of substantially higher absorbance by NATA in DMSO from ~294 to 310 nm. This extinction increase is attributed to the red-shifting of the L_a absorption band due to the hydrogen bonding of the indole N-H group with the dipolar, aprotic S═O group of DMSO. Because the dipole moment of the L_a state is larger than that of the L_b state (Pierce & Boxer, 1995), this interaction would preferentially stabilize the L_a state and move the L_a origin below that of the L_b state (Rehms & Callis, 1987; Strickland et al., 1970). This type of L_a-state lowering is also seen when a hydrogen-bonding solvent like butanol is mixed into a solution of indole or tryptophan model compound in a nonpolar solvent such as methylcyclohexane (Strickland et al., 1972, 1970). In these cases, one sees an increase in the extinction at the red edge of the absorption envelope. The deconvolution of the L_a and L_b contributions in the red tail of the low-temperature spectrum of NATA also reveals a distinct shoulder at ~295 nm due to a L_a vibronic band (Pierce & Boxer, 1995), whose size appears solvent dependent. Given the narrower linewidth of the 0—0 L_b vibronic band, these model compound studies argue that an absorbance increase at wavelengths above ~295 nm is indicative of a red-shifted L_a absorption.

Tryptophan residues inside proteins also exhibit these spectral properties. In the human tissue factor protein, the absorption spectra of two out of the four tryptophan residues display higher extinction above 295 nm compared to the spectrum of NATA in dioxane, while their 0—0 L_b peak positions are only slightly changed (Hasselbacher et al., 1995). In addition, the 0—0 L_a bands in the low-temperature absorption spectra of horseradish peroxidase and bovine/horse heart cytochromes have been resolved at ~300 and ~292 nm, respectively (Strickland et al., 1971). The difference of this L_a-shifted tryptophan absorption in a protein and a tryptophan in a weaker hydrogen-bonding environment would yield a band with substantial $\Delta\epsilon$ between 295 and ~310 nm as seen in the model difference spectrum of NATA in water and DMSO.

The comparison of the model compound and tryptophan-difference spectra enable us to infer the properties of the tryptophan environments in ground-state rhodopsin and in MII. The difference spectra of Trp^{126}, Trp^{161}, and Trp^{265} all show a band at ~294 nm, assigned to the differential 0—0 L_b band, indicating that they initially reside in a low dielectric environment. During the MI → MII transition or receptor activation (R → R*), the environments of Trp^{126} and Trp^{265} become polar, perhaps due to the accessibility of water at these sites, whereas the Trp^{161} environment becomes slightly less nonpolar.

The Trp^{265} environment in rhodopsin may be more nonpolar or polarizable compared to that of Trp^{126} because its difference peak appears red-shifted to 296 nm. This unique environment might be due to the proximity of Trp^{265} to the retinal chromophore, which has a large ground-state polarizability (Corsetti & Kohler, 1977; Ponder & Mathies, 1983). Results from several studies are consistent with the location of Trp^{265} in the retinal-binding pocket. First, the blue-shift of the chromophore absorption band in the W265Y, F, or A mutant (Nakayama & Khorana, 1990) indicates that Trp^{265} is close enough to interact with the retinal. Second, it seems to be one of the residues in steric proximity because introducing a phenylalanine at this position improves the stability of the pigment reconstituted with a 11-*cis*-retinal analogue with a locked C_{11}═C_{12} bond (Ridge et al., 1992). Lastly, Trp^{265} is one of the residues that cross-links with the β-ionone ring of a retinal analogue (Nakayama & Khorana, 1990; Zhang et al., 1994).

Chabre and Breton (1979) concluded that the L_b transition moment of a single tryptophan tilts toward the membrane plane during MI → MII conversion on the basis of the linear dichroism of the 296-nm difference band in the MII/Rho difference spectra of frog and bovine rhodopsins in native membranes. The assignment of this band to the absorption of a L_b transition is supported by linear dichroism of tryptophan model compounds (Albinsson et al., 1989) and consistent with the NATA difference spectra. The present tryptophan mutant data indicate that most of this signal originates from Trp^{265}. Therefore, we conclude that Trp^{265} is the residue whose indole plane changes orientation during the R → R* conformational transition. This result supports the initial hypothesis by Chabre and Breton that the tryptophan undergoing rotation is the one closest to the chromophore.

In addition to the bulk dielectric changes surrounding tryptophans, the larger $\Delta\epsilon$ at ~300 nm observed in the difference spectra of Trp^{126} and Trp^{265} is consistent with

changes in their hydrogen-bonding interactions during the R → R* transition. The Trp[126] difference spectrum contains a resolved peak at 302 nm, which is assigned to a difference of the shifted L_a transition. The Trp[265] difference spectrum clearly has differential absorbance assignable to L_a transition, but a separate peak is not resolved from the differential L_b band. Based on these observations, we conclude that the indole side chains of Trp[126] and Trp[265] are hydrogen bonded to another protein residue or group in the ground state of rhodopsin. The conformational change leading to MII formation or receptor activation alters tertiary interactions within the opsin and weakens these hydrogen-bond interactions. The FTIR spectrum of MII is also consistent with weaker hydrogen bonding and increased solvent accessibility of N-H group(s) which may belong to tryptophan residue(s) (Maeda et al., 1993; Kandori & Maeda, 1995). The results of this UV-absorption study suggest that the perturbed N-H group(s) may correspond to the indole N-H of either Trp[126], Trp[265], or both residues.

Earlier, the 286-nm difference band in the MII/Rho spectrum was explained as a tyrosine difference because its $\Delta\epsilon$ ($\sim$3500 M^{-1} cm^{-1}) was larger than that expected from a single tryptophan. Based on model NATA difference spectra (Figure 6C), the $\Delta\epsilon$ at $\sim$285 nm due to a secondary tryptophan difference peak is estimated to be $\sim$500 M^{-1} cm^{-1}. The $\Delta\epsilon$ due to a single tyrosine, which experiences the same change from a nonpolar to a polar environment, is $\sim$700 M^{-1} cm^{-1}. Therefore, the differential absorbance at 286 nm probably originates from 3−5 tyrosine residues that experience environmental perturbation concomitant with R → R* transition, with some contribution from the secondary difference band of Trp[265]. The rather large reduction of the 286-nm difference signal in the W265F/Y mutant suggests that the replacement of Trp[265] may indirectly inhibit the perturbations of some tyrosine residues.

Dynamics of Receptor Activation. The activation of rhodopsin represents a dynamic process that couples the chromophore photoisomerization to the reorganization of the cytoplasmic loop domains to conformations that are able to bind and to activate transducin. Biophysical studies on rhodopsin structure indicate that this process involves some alteration of the helix backbone conformation and interhelical contacts. Characteristic differences are detected in the infrared intensities and frequencies of the amide I and II vibrations between MII and rhodopsin. These observations are consistent with the perturbation of a number of peptide hydrogen bonds, which indicates a limited perturbation of secondary and tertiary structures (Klinger & Braiman, 1992). Recent analysis of the deconvoluted amide I bands between 1620 and 1700 cm^{-1} in rhodopsin and MII has interpreted the observed spectral differences in terms of a more extensive structural rearrangement that includes the alteration of the α-helical bundle structure, presumably due to distortions of some helix backbones, and a change in the secondary structures of solvent-exposed domains (Garcia-Quintana et al., 1995). However, the specific regions of the protein that participate in the dynamics of the activation process are not known.

In the absence of three-dimensional crystal structures of the R and R* conformations of rhodopsin, a molecular picture of the activation process must be reconstructed from information about changes in the local environments and structures of individual residues. It has been possible with

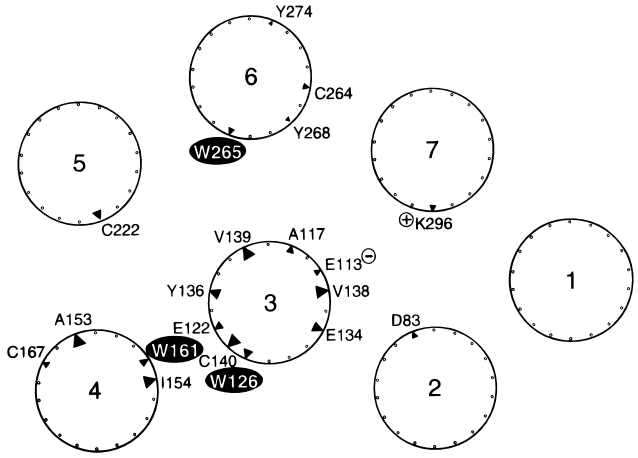

FIGURE 7: Schematic model of the seven-transmembrane helix arrangement in rhodopsin (Baldwin, 1993; Schertler & Hargrave, 1995) showing the probable locations of selected residues. The membrane-embedded tryptophans, Trp[126], Trp[161], and Trp[265], are highlighted by dark ovals. The view is of the membrane plane from the cytoplasm. The size of the triangle indicates the relative depth of the residue into the membrane. Larger triangles represent residues closer to the cytoplasmic membrane surface.

the combined use of site-directed mutagenesis and biophysical methods, such as FTIR and EPR spectroscopies, to identify amino acids whose environment and structure are altered upon MII formation (Figure 7). Most of these studies have focused on transmembrane helix 3, and the results suggest a significant perturbation of its disposition within the helix bundle. Glu[113], the counterion to the PSB group in rhodopsin, becomes protonated in MII (Jäger et al., 1994). In fact, one of the requirements for the initiation of the R → R* transition seems to be the neutralization of this carboxylate (Cohen et al., 1992; Zvyaga et al., 1994). There is also weakening of the hydrogen bonding of the carboxyl side chain of Glu[122](Fahmy et al., 1993). On the cytoplasmic surface of helix 3, EPR experiments detect a decrease in the steric interactions and increased mobility of the side chains of residues at positions 136, 138, 139, and 140, which form the putative tertiary contact sites of helix 3 with the neighboring helices (Farahbakhsh et al., 1995). The same study shows a smaller perturbation of side chains at positions 153 and 154 near the cytoplasmic border of helix 4. In addition, a conserved glutamic acid residue at position 134, near the cytoplasmic border of helix 3, becomes protonated (Arnis et al., 1994; Cohen et al., 1993). FTIR data show strengthening of hydrogen bonding by Asp[83] on helix 2 (Fahmy et al., 1993; Rath et al., 1993) and cysteine residue(s) (Rath et al., 1994).

Results relating to the Trp[126] and Trp[265] environments in rhodopsin and MII provide additional insight into the molecular details of the activation process. Trp[126] probably resides at or near the interface of helices 3 and 4 because it is positioned $\sim$3.6 helix turns from Glu[113]. In this orientation, the N-H group on its indole side chain could be hydrogen bonded to an acceptor group on helix 4. This interaction is broken or becomes significantly weaker in MII. Given that Trp[126] is also positioned $\sim$1 helix turn from Glu[122], the UV-absorption and FTIR data indicate a concerted disruption of hydrogen bonding by membrane-embedded side chains facing helix 4, which is coupled to the perturbation of the cytoplasmic surface residues (Tyr[136], Val[138], Val[139], Cys[140]) of helix 3. The evidence for extensive and concerted

perturbations of helix 3 between Glu^{122} and Cys^{140} suggests a motion of at least one-third of its length closest to the cytoplasm, which disrupts interhelical contact between helices 3 and 4, during the R → R* transition. This activity may account for the observed FTIR amide vibrational changes and may correspond to a rigid-body motion of the cytoplasmic end of helix 3 outward from the protein core as proposed by Farahbakhsh et al. (1995). It is interesting to note that the environment of Trp^{161}, which is predicted near the middle of bilayer at the interface of helices 3 and 4, changes less during the R → R* transition, supporting the idea that the dynamics is localized closer to the cytoplasm.

The perturbation of the Trp^{265} environment also points to the involvement of helix 6 in the activation process. Trp^{265} is positioned near the middle of the bilayer next to the retinal chromophore in a hydrophobic environment. This environment becomes more polar and the hydrogen bonding of its indole N-H becomes weaker when the protein switches to the active R* conformation. It is important to recognize that, in spite of the proximity of Trp^{265} to the chromophore, the Trp^{265} environment monitored by absorption changes is not sensitive to the isomerization or the deprotonation of the chromophore in the binding pocket, but is specifically affected by the general protein conformational change to the R* state. This implies that the Trp^{265} perturbation may reflect the fact that receptor activation involves dynamics of helix 6 to some degree.

Although the tyrosine assignments for the 286-nm difference band were not addressed in this study, the evidence for structural perturbations of helices 3 and 6 suggests that the environments of Tyr^{268} and Tyr^{274} on helix 6 and Tyr^{136} on helix 3 are likely to change. Differential absorptions by these residues may account for some of the difference signal at 286 nm in the MII/Rho spectrum. There is also evidence that the hydrogen bonding of at least one membrane-embedded cysteine (Cys^{167}, Cys^{222}, or Cys^{264}) is strengthened during the MI → MII conversion (Rath et al., 1994). Cys^{264} is a likely candidate given that the Trp^{265} environment experiences a strong perturbation. Cys^{222} is another possibile residue (Rath et al., 1994). On the other hand, only a minor change, if any, in the interactions of Cys^{167} is expected since it is located in the intradiscal half of helix 4 between Trp^{161} and Trp^{175}.

Summary. The UV-difference bands at 294 and 302 nm, which are observed in the MII/Rho-difference absorption spectrum, originate from the specific perturbations of the Trp^{126} and Trp^{265} environments during the R → R* conformational transition. Taken together with results from a variety of other biophysical studies, these tryptophan mutant data are consistent with a picture of rhodopsin activation which includes a collective or global rearrangement of opsin structure, that is mediated to some extent by dynamics of helices 3 and 6 within the helical bundle. This motion, possibly involving slight tilting of these helices, especially of the portion near the cytoplasmic membrane surface, probably induces transformations of the second and third cytoplasmic loops attached to helices 3 and 6, respectively, to their active conformations. Earlier mutagenesis studies have established the importance of these loops for the interaction with transducin (Franke et al., 1990, 1992; Ernst et al., 1995). In the protein interior, this reorganization disrupts the hydrogen-bonding interactions of Trp^{126} and Trp^{265} and increases the polarity around these tryptophans and several tyrosines.

ACKNOWLEDGMENT

We thank Kate Carroll for help with the construction of W126F and W161F mutant plasmids. We also thank May Han, Dr. Chris Min, Dr. Lenore Snyder, and Dr. Tanya Zvyaga for technical assistance and suggestions.

REFERENCES

Albinsson, B., Kubista, M., Nordén, B., & Thulstrup, E. W. (1989) *J. Phys. Chem. 93*, 6646−6654.
Arnis, S., & Hofmann, K. P. (1993) *Proc. Natl. Acad. Sci. U.S.A. 90*, 7849−7853.
Arnis, S., Fahmy, K., Hofmann, K. P., & Sakmar, T. P. (1994) *J. Biol. Chem. 269*, 23879−23881.
Baldwin, J. M. (1993) *EMBO J. 12*, 1693−1703.
Chabre, M., & Breton, J. (1979) *Photochem. Photobiol. 30*, 295−299.
Chan, T., Lee, M., & Sakmar, T. P. (1992) *J. Biol. Chem. 267*, 9478−9480.
Cohen, G. B., Oprian, D. D., & Robinson, P. R. (1992) *Biochemistry 31*, 12592−12601.
Cohen, G. B., Yang, T., Robinson, P. R., & Oprian, D. D. (1993) *Biochemistry 32*, 6111−6115.
Corsetti, J. P., & Kohler, B. E. (1977) *J. Chem. Phys. 67*, 5237−5243.
Ebrey, T. G. (1972) *Photochem. Photobiol. 15*, 585−588.
Ernst, O. P., Hofmann, K. P., & Sakmar, T. P. (1995) *J. Biol. Chem. 270*, 10580−10586.
Fahmy, K., & Sakmar, T. P. (1993) *Biochemistry 32*, 7229−7236.
Fahmy, K., Jäger, F., Beck, M., Zvyaga, T. A., Sakmar, T. P., & Siebert, F. (1993) *Proc. Natl. Acad. Sci. U.S.A. 90*, 10206−10210.
Fahmy, K., Siebert, F., & Sakmar, T. P. (1994) *Biochemistry 33*, 13700−13705.
Fahmy, K., Siebert, F., & Sakmar, T. P. (1995) *Biophys. Chem. 56*, 171−181.
Farahbakhsh, Z. T., Ridge, K. D., Khorana, H. G., & Hubbell, W. L. (1995) *Biochemistry 34*, 8812−8819.
Farrens, D. L., & Khorana, H. G. (1995) *J. Biol. Chem. 270*, 5073−5076.
Franke, R. R., König, B., Sakmar, T. P., Khorana, H. G., & Hofmann, K. P. (1990) *Science 250*, 123−125.
Franke, R. R., Sakmar, T. P., Graham, R. M., & Khorana, H. G. (1992) *J. Biol. Chem. 267*, 14767−14774.
Garcia-Quintana, D., Francesch, A., Garriga, P., de Lera, À., Padrós, E., & Manyosa, E. (1995) *Biophys. J. 69*, 1077−1082.
Hamm, H. E., Deretic, D., Arendt, A., Hargrave, P. A., Koenig, B., & Hofmann, K. P. (1988) *Science 241*, 832−835.
Hasselbacher, C. A., Rusinova, E., Waxman, E., Rusinova, R., Kohanski, R. A. L. W., Guha, A., Du, J., Lin, T. C., Polikarpov, I., Boys, C. W. G., Nemerson, Y., Konigsberg, W. H., & Ross, J. B. A. (1995) *Biophys. J. 69*, 20−29.
Henderson, R., Baldwin, J. M., Ceska, T. A., Zemlin, F., Beckmann, E., & Downing, K. H. (1990) *J. Mol. Biol. 213*, 899−929.
Hess, B., & Kuschmitz, D. (1979) *FEBS Lett. 100*, 334−340.
Hofmann, K. P. (1986) *Photobiochem. Photobiophys. 13*, 309−327.
Jäger, F., Fahmy, K., Sakmar, T. P., & Siebert, F. (1994) *Biochemistry 33*, 10878−10882.
Kandori, H., & Maeda, A. (1995) *Biochemistry 34*, 14220−14229.
Khorana, H. G. (1992) *J. Biol. Chem. 267*, 1−4.
Klinger, A. L., & Braiman, M. S. (1992) *Biophys. J. 63*, 1244−1255.
Maeda, A., Ohkita, Y. J., Sasaki, J., Shichida, Y., & Yoshizawa, T. (1993) *Biochemistry 32*, 12033−12038.
Mathies, R. A., Lin, S. W., Ames, J. B., & Pollard, W. T. (1991) *Annu. Rev. Biophys. Biophys. Chem. 20*, 491−518.
Min, K. C., Zvyaga, T. A., Cypess, A. M., & Sakmar, T. P. (1993) *J. Biol. Chem 268*, 9400−9404.
Nakayama, T. A., & Khorana, H. G. (1990) *J. Biol. Chem. 265*, 15762−15769.

Nakayama, T. A., & Khorana, H. G. (1991) *J. Biol. Chem. 266*, 4269−4275.
Nathans, J. (1990) *Biochemistry 29*, 9746−9752.
Pierce, D. W., & Boxer, S. G. (1995) *Biophys. J. 68*, 1583−1591.
Ponder, M., & Mathies, R. (1983) *J. Phys. Chem. 87*, 5090−5098.
Rafferty, C. N. (1979) *Photochem. Photobiol. 29*, 109−120.
Rafferty, C. N., Mullenberg, C. G., & Shichi, H. (1980) *Biochemistry 19*, 2145−2151.
Rath, P., DeCaluwé, L. L. J., Bovee-Geurts, P. H. M., DeGrip, W. J., & Rothschild, K. J. (1993) *Biochemistry. 32*, 10277−10282.
Rath, P., Bovee-Geurts, P. H. M., DeGrip, W. J., & Rothschild, K. J. (1994) *Biophys. J. 66*, 2085−2091.
Rehms, A. A., & Callis, P. R. (1987) *Chem. Phys. Lett. 140*, 83−89.
Resek, J. F., Farahbakhsh, Z. F., Hubbell, W. L., & Khorana, H. G. (1993) *Biochemistry 32*, 12025−12032.
Resek, J. F., Farrens, D., & Khorana, H. G. (1994) *Proc. Natl. Acad. Sci. U.S.A. 91*, 7643−7647.
Ridge, K. D., Bhattycharya, S., Nakayama, T. A., & Khorana, H. G. (1992) *J. Biol. Chem. 267*, 6770−6775.
Ridge, K. D., Lu, Z., Liu, X., & Khorana, H. G. (1995) *Biochemistry 34*, 3261−3267.
Sabés, M., Duñach, M., Mañosa, J., Morros, A., & Padrós, E. (1984) *Photobiochem. Photobiophys. 8*, 97−101.
Sakmar, T. P., Franke, R. R., & Khorana, H. G. (1989) *Proc. Natl. Acad. Sci. U.S.A. 86*, 8309−8313.
Schertler, G. F. X., & Hargrave, P. A. (1995) *Proc. Natl. Acad. Sci. U.S.A. 92*, 11578−11582.
Strickland, E. H., Horwitz, J., & Billups, C. (1970) *Biochemistry 9*, 4914−4921.
Strickland, E. H., Horwitz, J., Kay, E., Shannon, L. M., Wilchek, M., & Billlups, C. (1971) *Biochemistry 10*, 2631−2638.
Strickland, E. H., Billups, C., & Kay, E. (1972) *Biochemistry 11*, 3657−3662.
Valeur, B., & Weber, G. (1977) *Photochem. Photobiol. 25*, 441−444.
Wald, G., & Brown, P. K. (1953) *J. Gen. Physiol. 37*, 189−200.
Wu, S., Jang, D.-J., El-Sayed, M. A., Marti, T., Mogi, T., & Khorana, H. G. (1991) *FEBS Lett. 284*, 9−14.
Yoshizawa, T. (1992) *Photochem. Photobiol. 56*, 859−867.
Zhang, H., Lerro, K. A., Yamamoto, T., Lien, T. H., Sastry, L., Gawinowicz, M. A., & Nakanishi, K. (1994) *J. Am. Chem. Soc. 116*, 10165−10173.
Zhukovsky, E. A., & Oprian, D. D. (1989) *Science 246*, 928−930.
Zvyaga, T. A., Min, K. C., Beck, M., & Sakmar, T. P. (1993) *J. Biol. Chem. 268*, 4661−4667; Correction: (1994) *J. Biol. Chem. 269*, 13056.
Zvyaga, T. A., Fahmy, K., & Sakmar, T. P. (1994) *Biochemistry 33*, 9753−9761.

BI960858U